JOURNAL OF MATERIALS SCIENCE 23 (1988) 1159–1163

Electrical properties of plasma-sprayed yttria-stabilized zirconia films

G. CHIODELLI, A. MAGISTRIS,
CSTE-CNR e Dipartimento di Chimica Fisica, Università di Pavia, viale Taramelli 16, 27100 Pavia, Italy

M. SCAGLIOTTI, F. PARMIGIANI
CISE-Tecnologie Innovative S.p.A., via Reggio Emilia 39, 20090 Segrate (Milano), Italy

Yttria-stabilized zirconia films, 100 to 200 μm thick, were prepared by plasma spraying. The electrical properties were investigated by complex impedance spectroscopy. The results are compared with those obtained on sintered pellets prepared with the same powders used for spraying and on commercial single crystals. The ionic conductivity and the activation energies of sprayed films and single crystals are found to be very similar, and no grain-boundary effect is observed in the film complex impedance plots. These results are explained by the high density and purity of the sprayed films.

1. Introduction

Thin film electrolytes have recently gained attention for their technological application in fuel cells [1], sensors [2] and electrochemical devices [3]. Different deposition techniques, including physical vapour deposition, chemical vapour deposition and plasma spraying, are suitable to produce such materials. However, the film properties strongly depend on the deposition parameters. Above all, the film stoichiometry and structure, which are strongly related to the ionic conductivity, can be different from those of the starting materials.

Mixed oxide systems like stabilized zirconia, are of particular interest from this point of view. Ionic conductivity in zirconia-based electrolytes depends on the structure, the microstructure and the impurity content [4–6]. The crystallographic structure is controlled by the stabilizing oxide amount, by the deposition parameters and by the thermal treatment of the films. The deposition process and the thermal treatment parameters also affect the film microstructure, i.e. the grain size, the film density and the grain boundaries. Impurities can be introduced either as sintering aids in the powders (SiO_2, Al_2O_3, etc.) or as contaminations during the film deposition. These facts and the interesting results obtained on high-temperature solid oxide fuel cells with plasma-sprayed zirconia electrolytes [7] have stimulated the present work. The electrical properties of plasma-sprayed zirconia electrolytes were investigated by impedance spectroscopy, and the results are compared with those obtained on sintered pellets, prepared with the same powders used for spraying, and on single crystals. The structural properties of the same films are reported in detail elsewhere [8].

The analysis of the impedance spectra shows that plasma-sprayed films and single crystals exhibit ionic conductivity of the same order of magnitude and no grain-boundary effects. This is due to the high density, large grain size and purity of the sprayed zirconia films. From the present data the plasma spraying technique appears to be particularly suitable to prepare yttria-stabilized zirconia electrolytes.

2. Experimental techniques

2.1. Sample preparation

The samples studied in the present work are plasma-sprayed films, sintered pellets and single crystals of yttria-stabilized zirconia. Films and sintered pellets were prepared using the same powders, while the single crystals were supplied by Ceres Corporation (USA).

The fine ZrO_2 and Y_2O_3 powders 99% pure, supplied by Merck and certified silica free, were mixed in the compositions ZrO_2–(8, 10, 12 mol %) Y_2O_3, milled in a tungsten carbide mill with tungsten carbide balls, and then stabilized by heating in air at 1550° C for 24 h.

Films, 100 to 200 μm thick, were sprayed in air using argon as plasma gas. This technique and the experimental procedure are described in detail elsewhere [8]. To improve the density, the films were sintered in vacuum at 2000° C (sample 1) or 2100° C (sample 2) for 3 h and then annealed in air at 1450° C for 3 h to restore the oxygen stoichiometry.

Part of the stabilized powders was used to prepare pellets sintered in air at 1700° C for 24 h. Stabilized zirconia single crystals (ZrO_2–4.5, 12, 18 and 24 mol % Y_2O_3) were grown by skull melting. Specimens, 1.5 mm thick, were cut from the base of columnar-shaped crystals and polished by using diamond pastes.

2.2. Sample characterization

The samples were analysed in order to determine the chemical composition, the density, the microstructure and the crystallographic structure [8].

0022–2461/88 $03.00 + .12

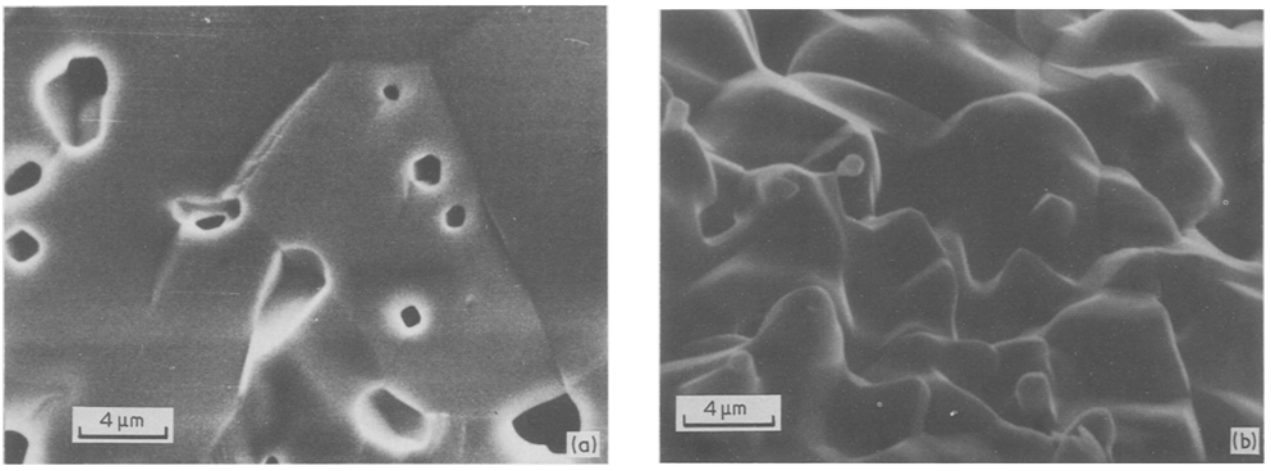

Figure 1 Typical scanning electron microphotographs of a plasma-sprayed film: (a) cross section and (b) surface.

The yttrium/zirconium ratio of the films was tested by proton induced X-ray emission (PIXE) [8] and the measured compositions are reported in Table I. Slight deviations from the nominal composition are observed except for the ZY8-2 sample where the Y/Zr ratio is strongly increased [8]. The microstructure of the sprayed films was investigated by optical microscopy and scanning electron microscopy (SEM). As shown in Fig. 1, the films appear dense, with large grain size and a few micrometre-sized pores. The average grain size, measured on polished and etched film cross-sections, is about 20 μm.

The crystallographic structure was investigated by X-ray diffraction (XRD) and Raman spectroscopy. All the samples appear completely stabilized in the cubic phase except for the ZrO_2–4.5 mol % Y_2O_3 single crystal. The Raman spectrum of this crystal exhibits typical bands due to the tetragonal phase [8] and a broad background, which indicates the presence of the cubic phase, while the presence of monoclinic zirconia can be excluded on the basis of the Raman results. Lattice parameters of plasma-sprayed films, sintered pellets and single crystals, measured from X-ray reflections of the (4 0 0) planes, are reported in Table I. These lattice parameters were used to calculate the sample densities, taking into account the vacancies formed by the yttria stabilizer (Table I) [9, 10].

The sample density was measured at 20° C by the Archimedes technique using distilled water and ethanol. The results, estimated to be precise to $\pm 1\%$, are reported in Table I.

2.3. Electrical measurements

Electrical conductivity was measured by a complex impedance method. A Solartron 1174 frequency response analyser, equipped with a high impedance adaptor ($10^{12}\Omega$, 6 pF), was used in the frequency range between 0.01 Hz and 1 MHz. The experimental apparatus was interfaced with a microcomputer in order to process the data.

Platinum electrodes, 300 nm thick, were sputtered on the samples by means of a Balzer Sputron II apparatus. The cell constant of the plasma-sprayed films, $K = l/S$, where S is the surface area and l the film thickness, was estimated to within $\pm 10\%$ of its value. The measurements for each composition of plasma-sprayed films were repeated four times.

3. Results and discussion

3.1. Complex impedance analysis

The frequency dispersion measurements were analysed according to the equivalent circuit reported in Fig. 2 [4]. A similar circuit has been proposed for the "brick layer" model [11] and adopted by several authors [5, 12] in order to interprete the electrical response of polycrystalline and single-crystal yttria-stabilized zirconia electrolytes. In the same figure

TABLE I

Sample		Y_2O_3 (mol %)	Lattice parameter exp. (nm)	Density		
				calc. ($g\,cm^{-3}$)	exp. ($g\,cm^{-3}$)	exp/calc (%)
Sintered pellets		8	0.5139	5.95	5.50	92
		10	0.5141	5.93	5.50	92
		12	0.5143	5.91	5.53	93
Films	ZY8-1	9.5	0.5132	5.97	5.85	98
	ZY10-2	10.7	0.5134	5.95	5.81	98
	ZY12-1, -2	11.1	0.5135	5.94	5.81	98
	ZY8-2	14.5	0.5150	5.86	5.78	98
Single crystals		4.5	0.5123	6.04	6.05	100
		12	0.5150	5.89	5.90	100
		18	0.5164	5.79	5.82	100
		24	0.5177	5.71	5.72	100

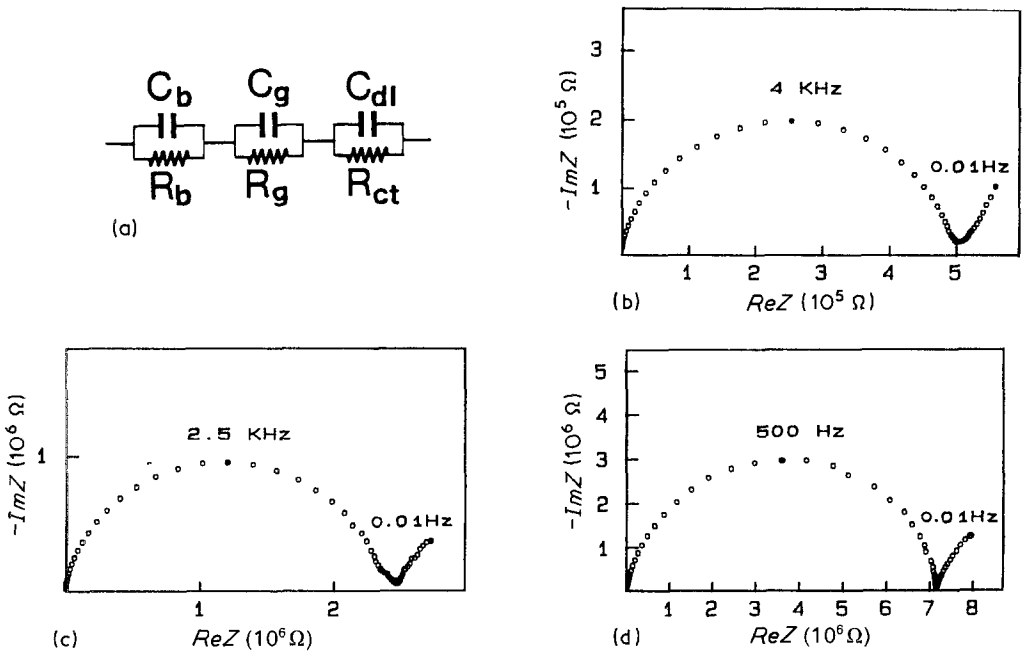

Figure 2 Equivalent circuit for the electrical response of polycrystalline ceramic samples (a), typical complex impedance plots, at the same temperature (220° C), of a (b), plasma-sprayed film sintered pellet (c) and single crystal (d).

the impedance spectra of a sprayed film, a sintered pellet and a single crystal with the same nominal composition, are reported at $T = 220°\,C$. The plasma-sprayed film and the single crystal are characterized by only one arc due to the bulk conductivity $\sigma_b = K/R_b$, where K is the cell constant. In the sintered pellet a distortion of the electrolyte arc in the low frequency regions suggests the presence of a second arc, associated with grain-boundary effects. For all the samples the depression of the semicircles has a temperature independent value of 10 to 15° C. The arc in the lower frequency region, due to electrode effects, less evident in Fig. 2, becomes dominant at higher temperatures.

The relatively small grain-boundary resistance observed in sintered pellets is consistent with the results reported for samples with low porosity, low-impurity content and well-developed microstructure [6, 11]. The absence of grain-boundary contributions in plasma-sprayed films, prepared with the same powders used for sintered pellets, can be explained by the high-purity and/or relative density of the films (see Table I).

As expected, transparent cubic single crystals, free of micro-inhomogeneity gave only one well-shaped arc due to the bulk conductivity, whereas in the ZrO_2–4.5 mol % Y_2O_3 opaque crystal, where tetragonal and cubic phases are present, the arc appears quite distorted, in agreement with previously reported results [6, 12, 13]. For all samples, in the high-frequency region at low temperature, a parallel capacitance C_p of the order of tens of pF does not vary significantly with the frequency. Therefore, according to the proposed equivalent circuit, these values were attributed to the high-frequency limiting capacitance of the bulk material. The relative dielectric constants ε_r were calculated from the expression $\varepsilon_r = C_p K/e_0$, were e_0 is the vacuum permittivity ($8.854 \times 10^{-14}\,F\,cm^{-1}$). Data of ε_r obtained from capacitance measurements at 1 MHz, are reported in Table II.

TABLE II

Y_2O_3 (mol %)	ε_r	Low temperature		High temperature	
		E_a (eV)	A ($\Omega^{-1}\,cm^{-1}\,K$)	E_a (eV)	A ($\Omega^{-1}\,cm^{-1}\,K$)
Sintered pellets					
8	29	1.07	4.6×10^6	0.80	1.9×10^5
10	26	1.13	9.6×10^6	0.76	7.4×10^4
12	26	1.19	1.3×10^7	0.67	2.1×10^4
Films					
9.5	34	1.09	8.7×10^6	0.74	1.1×10^5
10.7	33	1.13	2.3×10^7	0.72	1.0×10^5
11.1	30	1.10	1.4×10^7	0.73	1.1×10^5
14.5	30	1.22	2.7×10^7	0.86	1.5×10^5
Single crystals					
4.5	33	0.96	8.8×10^5	0.78	8.5×10^4
12	29	1.26	3.2×10^7	0.80	9.0×10^4
18	24	1.43	2.1×10^7	1.19	1.1×10^6
24	23	1.47	1.9×10^7	1.18	5.4×10^5

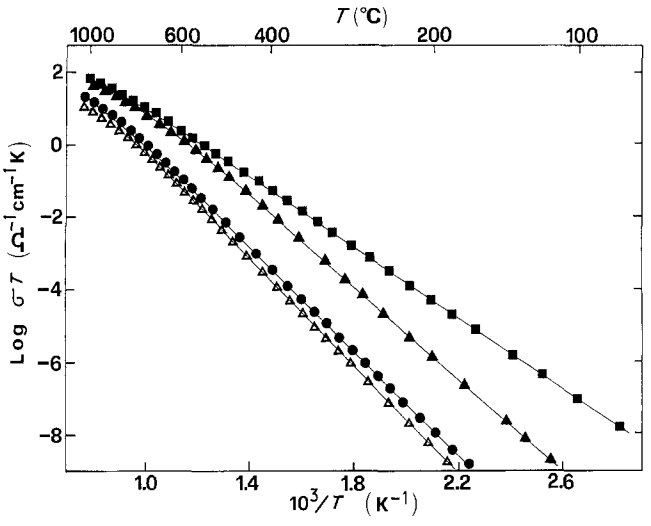

Figure 3 Plots of conductivity against temperature of single crystals with different Y_2O_3 content: (■) 4.5 mol %; (▲) 12 mol %; (●) 18 mol %; (△) 24 mol %.

3.2. Conductivity

According to the general expression $\sigma T = A \exp(-E_a/k_B T)$, the activation energy E_a and the pre-exponential factor A were obtained from plots of log $\sigma_b T$ against $1/T$ using the least square methods.

Figs 3 and 4 show the Arrhenius plots of single-crystal and plasma-sprayed samples, respectively. Similar results were obtained with sintered pellets. Two straight line portions, with different slopes, are observed for all the samples. This dependence of the activation energy on the temperature, is generally explained with the formation of dopant cation–vacancy pairs at low temperatures [4, 6]. Values of A and E_a obtained in the low ($< 550°$ C) and high ($> 650°$ C) temperature regions are reported in Table II for all the investigated samples.

At high temperatures the activation energy ranges from 0.7 to 0.8 eV below 12 mol % yttria, while for higher yttria content (18 to 24 mol %) the values are around 1.2 eV. These results are in agreement with those reported in literature [6, 14]. In the low-temperature region, where microstructure, impurity level and association phenomena are important, some differences are observed, as shown in Fig. 5, where E_a and A values are plotted as a function of the yttria content. As a general trend, in the cubic phase E_a increases with the Y_2O_3 content, whereas A remains quite independent on composition; A and E_a values are lower in the ZrO_2–4.5 mol % Y_2O_3 single crystal, with tetragonal structure. The same result was reported by Ikeda *et al.* [14] for single crystals in a wide composition range. Plasma-sprayed films and sintered pellets showed A and E_a values very close, only slightly lower than those observed for single crystals with the same composition.

In Fig. 6, isothermal bulk conductivities plotted against yttria content for plasma-sprayed films, sintered pellets and single crystals, are compared at three selected temperatures. The occurrence of a maximum of conductivity around the minimum Y_2O_3 level (6 to 7 mol %) required to stabilize the cubic fluorite structure is confirmed, in agreement with the results previously reported for polycrystalline samples and single crystals [4].

It is important to note that plasma-sprayed films exhibit the same or little better bulk conductivity with respect to sintered and single-crystal samples of the same compositions.

In conclusion, a film of yttria-stabilized zirconia prepared by plasma spraying and densified at high temperature, exhibits electrical properties similar to those of single crystals growth by skull melting and they can be used, as solid electrolytes, in electrochemical devices. However, further studies will be necessary in order to improve the as-sprayed film density and avoid high-temperature sintering which

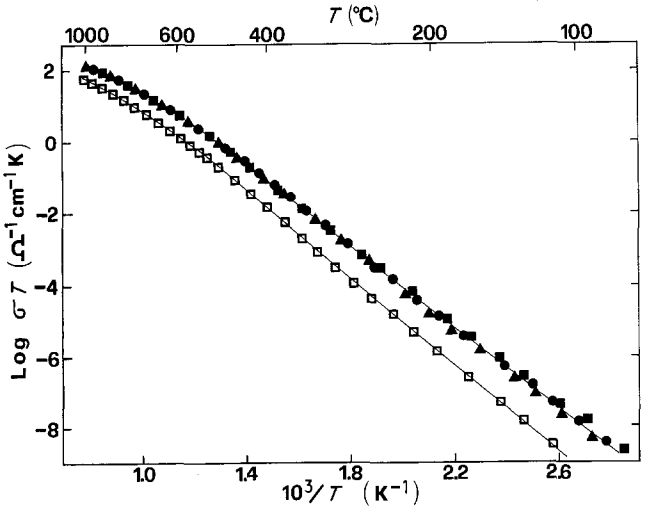

Figure 4 Plots of conductivities against temperature for different plasma-sprayed films: (■) ZY8-1; (▲) ZY10-1; (●) ZY12-1; (□) ZY8-2.

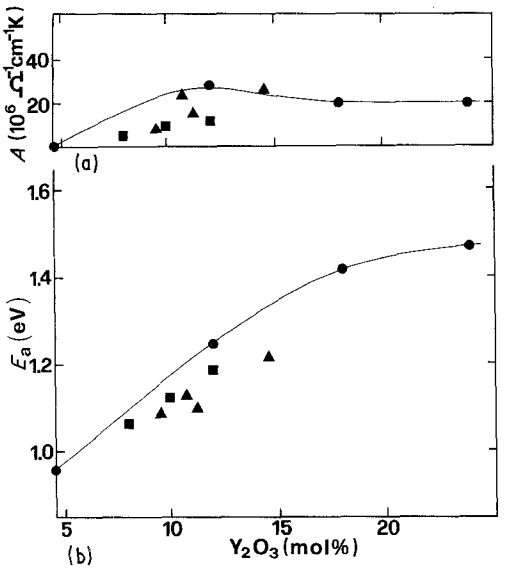

Figure 5 Pre-exponential factor, A, and activation energy E_a plotted against Y_2O_3 content for single crystals (●), sintered pellets (■) and plasma-sprayed films (▲). The full line, shown to guide the eye, follows the general trend reported in the literature for yttria-stabilized zirconia single crystals.

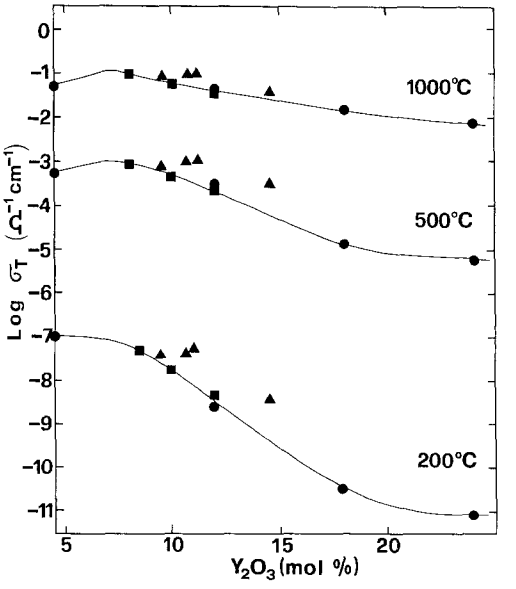

Figure 6 Isothermal conductivities plotted against Y_2O_3 content at three selected temperatures for single crystals (●), sintered pellets (■) and plasma-sprayed films (▲). The full line, shown to guide the eye, follows the general trend reported in the literature for yttria-stabilized zirconia single crystals.

cannot be carried out on multilayer fuel cell stacks. In particular, vacuum plasma spray deposition should be tested.

Acknowledgements

We wish to thank D. Richon (Battelle-Geneva) for plasma sprayed film preparation. The work was supported by the "Progetto Finalizzato Energetica II", CNR-ENEA, grant ENEA n.556/86.

References

1. H. S. ISAACS, *Adv. Ceram.* **3** (1981) 406, and references therein.
2. G. VELASCO, *Solid State Ionics* **9, 10** (1983) 783.
3. S. CHANDRA, "Superionic Solids" (North Holland, Amsterdam, 1981) Ch. 6, and references therein.
4. J. A. KILNER and B. C. H. STEELE, in "Non-Stoichiometric Oxides", edited by O. T. Sørensen (Academic, London, 1981) p. 233.
5. M. J. VERKERK, A. J. A. WINNUBST and A. J. BURGGRAAF, *J. Mater. Sci.* **17** (1982) 3113.
6. S. BADWAL, *ibid.* **19** (1984) 1767.
7. S. NAGATA, Y. OHNO, Y. KASUGA, Y. KAGA and H. SATO, Proceedings 19th Intersoc. Energy Conv. Eng. Conference, San Francisco 19 August 1984, Vol. 2 (Am. Nucl. Soc.) p. 827.
8. M. SCAGLIOTTI, F. PARMIGIANI, G. SAMOGGIA, G. LANZI and D. RICHON, *J. Mater. Sci.*, in press.
9. R. P. INGEL and D. LEWIS III, *J. Amer. Ceram. Soc.* **64** (1986) 325.
10. V. I. ALEKSANDROV, G. E. VAL'YANO, B. V. LUKIN, V. V. OSIKO, A. E. RAUTBORT, V. M. TATARINTSEV and V. N. FILATOVA, *Izv. Akad. Nauk SSSR Neorg. Mater.* **12** (1976) 273.
11. T. VAN DIJK and A. J. BURGGRAAF, *Phys. Status Solidi (a)* **63** (1981) 229.
12. N. BONANOS and E. P. BUTLER, *J. Mater. Sci. Lett.* **4** (1985) 561.
13. N. BONANOS, R. K. SLOTWINSKI, B. C. H. STEELE and E. P. BUTLER, *ibid.* **3** (1984) 245.
14. S. IKEDA, O. SAKURAI, K. UEMATSU, N. MIZUTANI and M. KATO, *J. Mater. Sci.* **20** (1985) 4593.

Received 8 June
and accepted 20 August 1987